

PERFORMANCE OF TACTICAL VHF FH-RADIOS REFERRING TO RADIO CHANNEL MEASUREMENTS

Gerald L. Berger
Helmut Safer, Franz Seifert

University of Technology Vienna, Applied Electronics Laboratory
A-1040 Wien, Gusshausstr. 27 / 3592, Austria, Europe
e-mail: berger@ps1.iaee.tuwien.ac.at

ABSTRACT

The performance of VHF frequency hopping (FH) radios with different synchronization philosophies and datarates is investigated, based on a statistical radio channel model which takes into account the spatially inhomogeneous distribution of partial waves. The channel parameters are gained from VHF wideband channel measurements in mountainous terrain. For the simulation we use a binary frequency shift keying (BFSK) modulation with 20 and 80 kbit/sec and a non-coherent matched Filter (MF) receiver with a maximum likelihood decision. All functional blocks in the communication system are represented in the baseband where the dependence on the carrier frequency is included in the channel model. Due to multipath propagation, the optimum sampling time at the output of the receiver's MF changes for each carrier frequency and for different receiver positions. The simulation results show the difference in the bit error rate (BER) for different data rates of a slow FH radio system with and without synchronizing each hop.

INTRODUCTION

Usually it is assumed that a spread spectrum system has an advantage in a multipath environment compared to a narrow band system. This can be seen if we consider the channel transfer function. FH over a bandwidth much larger than the coherence bandwidth guarantees a residual BER which is the mean BER averaged over all carrier frequencies. But this estimation of the BER assumes perfect synchronization of all hops. If the radio would be operated in an additive white Gaussian noise (AWGN) channel, an initial synchronization would be sufficient, because the propagation delay for a radio signal is the same for each hop frequency. But under multipath conditions with more than one echo the time of arrival of the radio signal can not be determined in advance for each frequency. To simulate the performance (BER) of a radio system under nearly real conditions, a channel model referring to measurements is needed which includes the effects of fading and propagation delays.

CHANNEL DESCRIPTION

For the evaluation of channel measurements we use the time-variant channel description, first introduced by Bello [Bel63], which is commonly accepted, especially under the assumption of "wide sense stationary uncorrelated scattering" (WSSUS). For the channel measurements the transmitter of the used channel sounder [Ber97] is located at a fixed position while the channel impulse response is recorded continuously by the receiver at discrete positions $x = \{x_1, x_2, \dots, x_M\}$ along a line at distances $\Delta x = x_m - x_{m-1}$ smaller than half a wavelength. Therefore the received signal at the output of the channel sounder can be described as

$$y(\tau, x) = \sum_n \alpha_n(x) s(\tau - \tau_n(x)) \quad (1)$$

where $\alpha_n(x)$ denotes the attenuation of the signal components at delay τ_n and at the receiver position x . For further considerations on the measurement data we use the complex envelope representation of $y(\tau, x)$:

$$\tilde{y}(\tau, x) = y_c(\tau, x) + jy_s(\tau, x) = \sum_n \tilde{\alpha}_n(x) \cdot \tilde{s}(\tau - \tau_n(x)) \quad (2)$$

with $\tilde{\alpha}_n(x) = \alpha_n(x) e^{-j2\pi f_c \tau_n(x)}$ and $\tilde{s}(\tau) = s_c(\tau) + js_s(\tau)$. The complex envelope representation of the output signal $\tilde{y}(\tau, x)$ is a sufficient channel description $\tilde{h}(\tau, x) = \tilde{y}(\tau, x)$ for radio systems within the sounding bandwidth. To calculate the scattering function $P_s(\cos \alpha, \tau)$ from the position-variant impulse response, we perform the Fourier Transform on $\tilde{h}(\tau, x)$ referring to x with respect to the wavelength λ_c of the sounding signal. The scattering function is a very compact description of the radio channel which enables the location of the scatterers within the radio channel.

CHANNEL MEASUREMENT

For further considerations we use a channel impulse response which was recorded in the mountainous area of Ennstal, which belongs to the Austrian Alps. Figure 2 shows the magnitude of the position-variant complex impulse response $\tilde{h}(\tau, x)$, measured at 60 MHz. With a

sounding bandwidth of 6 MHz we get a delay resolution of 417 nsec [Ber97].

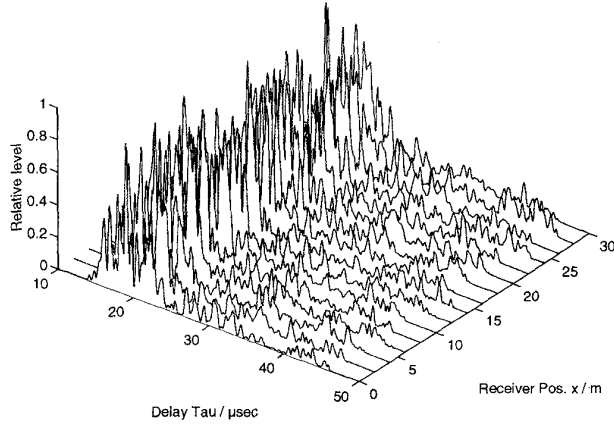


Figure 1: Magnitude of the position-variant complex impulse response at 60 MHz

For the angle of incidence α and the delay τ the resulting scattering function $P_S(\cos \alpha, \tau)$ is depicted in Figure 2.

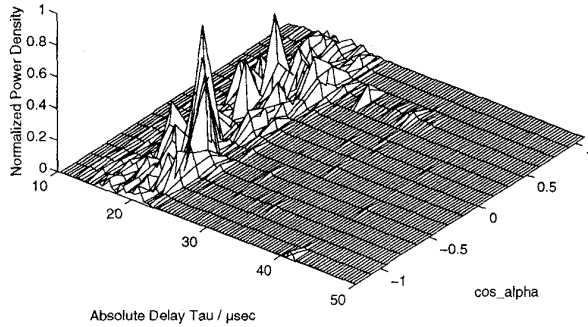


Figure 2: Scattering function related to Figure 1.

CHANNEL MODEL

To extract the parameters from the scattering function we used a simplified version of the method proposed by Blanz [Bla96]. Since the echoes can not be appointed to a discrete scatterer we divide the scattering function to several cells with a size of $\Delta\tau$ and $\Delta\cos(\alpha)$. The energy content of each cell is

$$E_{\tau_C, \cos \alpha_C} = \int_{\tau_C - \frac{\Delta\tau}{2}}^{\tau_C + \frac{\Delta\tau}{2}} \int_{\cos \alpha_C - \frac{\Delta \cos \alpha}{2}}^{\cos \alpha_C + \frac{\Delta \cos \alpha}{2}} P_S(\cos \alpha, \tau) \cdot d\tau \cdot d\cos \alpha. \quad (3)$$

For the proposed channel model each cell of the scattering area is represented by a number of uniformly distributed scattering points with reflection coefficient one. Here the number of discrete scattering points is proportional to the energy content $E_{\tau_C, \cos \alpha_C}$. To get a realistic behavior of the channel model, the number of scattering points should be high. On the other hand a large number increases the computing effort during a simulation. A compromise between this two demands leads us to a numbers of 10 scattering points for the cell with the highest energy ($E_{\tau_C, \cos \alpha_C, \max}$). The number of scattering points for the other cells are

$$N_{\tau_C, \cos \alpha_C} = \text{int} \left(\frac{10 \cdot E_{\tau_C, \cos \alpha_C}}{E_{\tau_C, \cos \alpha_C, \max}} \right), \quad (4)$$

where $\text{int}(x)$ is the integer of x . Figure 3 shows the number of scattering points in each cell for the measured scattering function (Figure 2).

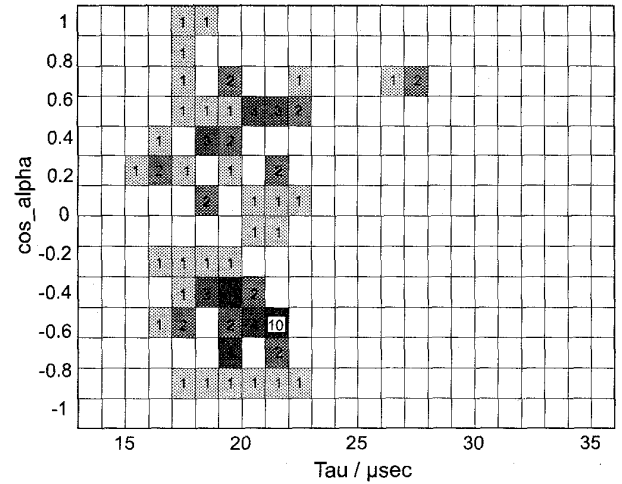


Figure 3: Number of scattering points for each cell

To get a relation to the physical scattering areas, each scattering point can be transformed to a Cartesian coordinate system under the assumption of a single reflection. With the help of a map the ambiguity of the angle of incidence α can be determined in most cases. Figure 4 shows the generated scattering points according to (4) with an underlying map. It can be seen that the diffuse reflection is caused by the surrounding mountains. From this constellation the channel impulse response can be calculated for each receiver position R_x as sum of Dirac's functions over all scattering points (N).

$$h(\tau, x) = \sum_{n=1}^N \delta(\tau - \tau_n(x)) \quad (5)$$

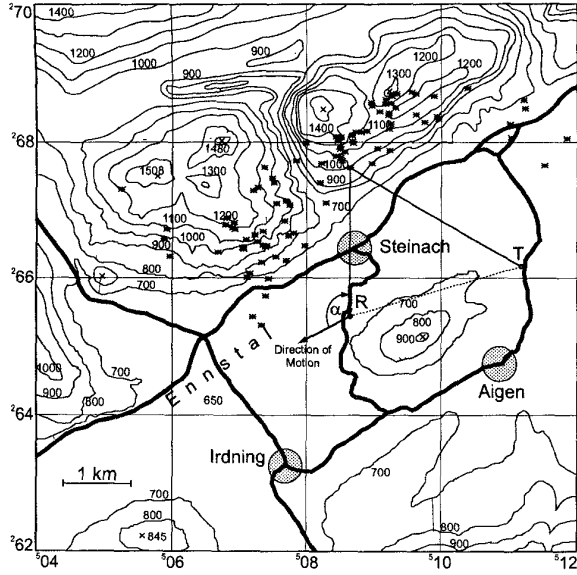


Figure 4: Randomly generated scattering points according to Figure 3

If we denote the positions of the receiver (\vec{R}_x), the transmitter (\vec{T}) and the scatterers (\vec{S}_n) as vectors and assume that the speed of the radio signal in the atmosphere is equal to the speed of light (c_0) the delay time for the reflected waves is

$$\tau_n(x) = \frac{|\vec{T} - \vec{S}_n| + |\vec{R}_x - \vec{S}_n|}{c_0}. \quad (6)$$

For the use in a simulation, we transform $h(\tau, x)$ to the complex envelope representation

$$\tilde{h}(\tau, x) = \sum_{n=1}^N \delta(\tau - \tau_n(x)) \cdot e^{-j2\pi f_c \tau_n(x)}. \quad (7)$$

This channel model allows us to generate an unlimited number of channel impulse responses depending on the receiver position R_x and the carrier frequency f_c . Since the effects of fading and propagation delays are automatically included, it allows us to simulate a radio system under realistic channel conditions. For the investigated radio system we generated $\tilde{h}(\tau, x)$ with 64 discrete receiver positions and for carrier frequencies from 59 to 61 MHz in steps of 25 kHz.

RADIO SYSTEM

To get comparable simulation results to existing tactical VHF-radios we use a BFSK modulation in the transmitter and a non-coherent MF-concept in the receiver [Ber98]. The overall blockdiagram is given in Figure 5. In the first stage of the transmitter a random binary data stream $A_k \in \{-1, +1\}$ is generated as input signal for the binary frequency shift keyed (BFSK) modulator. In order to recover \hat{A}_k , the output of the matched filter must be sampled at the appropriate instants t_k , where the estimate of the system delay D_s has to be determined before [Jer92]. This can be done for instance by a preamble with good autocorrelation properties. For the synchronization we transmit two FSK-pulses, one representing a „-1“ and another representing a „+1“. In both cases we calculated the difference of the MF output signals and set D_s to the time where the sum of both transmissions shows a maximum to get the optimum estimation ($D_{s,opt}$).

$$g_{sync}(t) = (|\tilde{g}_{0,-1}(t)| - |\tilde{g}_{1,-1}(t)|) + (|\tilde{g}_{1,+1}(t)| - |\tilde{g}_{0,+1}(t)|) \quad (8)$$

$$g_{sync}(D_{s,opt}) = \max\{g_{sync}(t)\} \quad (9)$$

SIMULATION

The data rate was set to 20 kbit/sec ($T_b = 50 \mu s$), which is typical for the on the air data rate of tactical VHF-FH-radios. For the simulation the system sampling time was set to $T_s = T_b/8$. Therefore the estimated system delay D_s can be varied in discrete steps of $T_s = 6.25 \mu s$. The normalized relative system delay D can be written as

$$D = (D_s - D_0)/T_s \quad (10)$$

where D_0 is a constant system delay. The simulation (Figure 6) shows that the optimum sampling time D_{opt} varies, depending on the receiver position and the carrier frequency. The optimum sampling time varies about $2T_s = 12.5 \mu s$ which is in the range of the maximum excess delay of the measured impulse response (Figure 1). In a following Monte Carlo simulation the bit error rate $BER_D(E_b/N_0)$ was estimated for all occurring delays ($D = 0.2$) and for the optimum

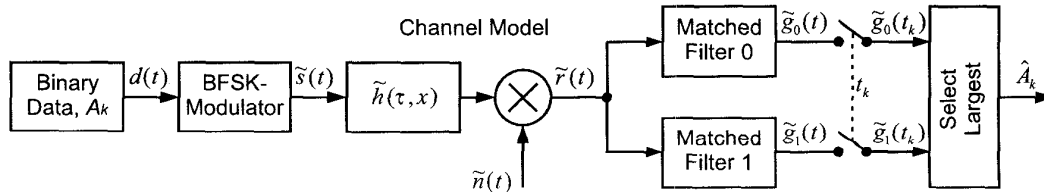


Figure 5: Simulation configuration

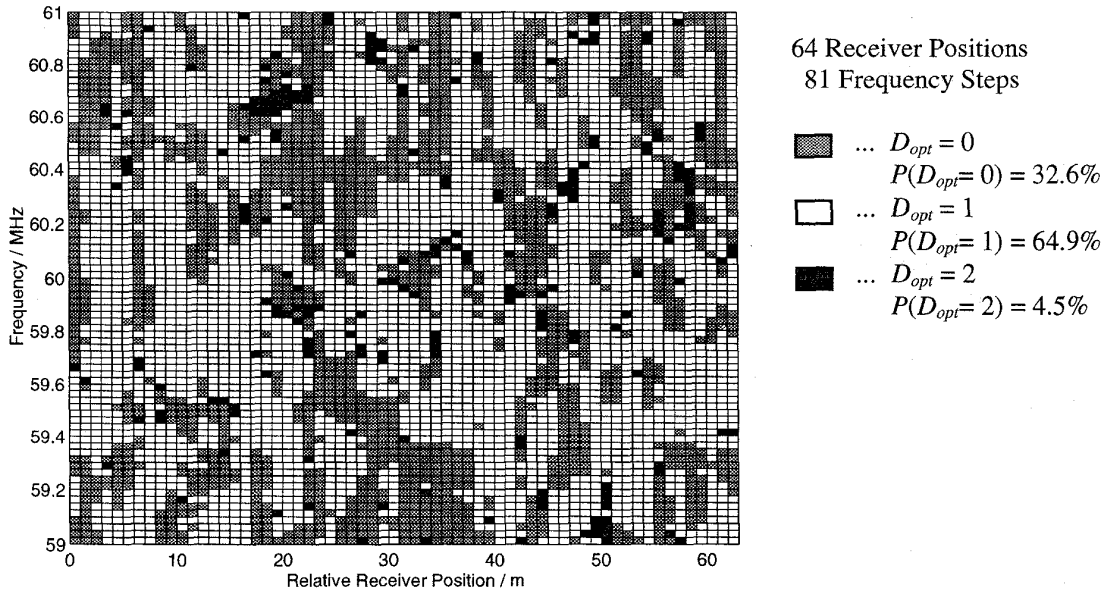


Figure 6: Optimum sampling time D_{opt} depending on f_c and R_x .

sampling time D_{opt} . The simulation results (Figure 7) show that the BER for all possible delays in comparison with analytic results for a Rayleigh and an AWGN channel. Due to the inter symbol interference (ISI) which causes an irreducible error floor the BER varies very strongly on the bit synchronization.

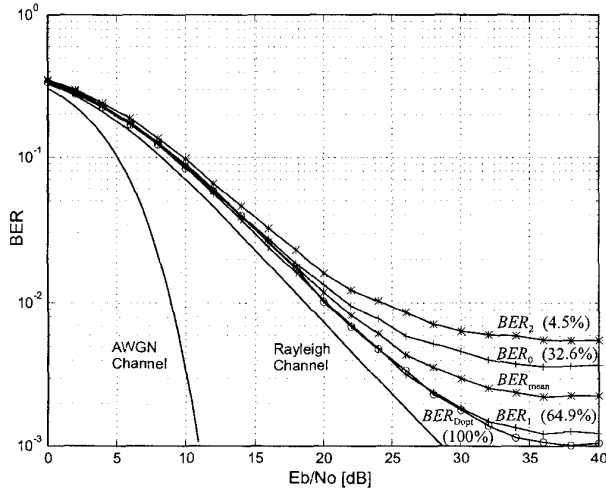


Figure 7: BER for all possible delays

For radio systems which synchronize randomly at one frequency, the error floor varies from $1.2 \cdot 10^{-3}$ to $5.6 \cdot 10^{-3}$ depending on the synchronization frequency and the receiver position. The resulting mean BER (BER_{mean}) can be calculated from the BERs with fixed synchronization time ($BER_{0...2}$).

$$BER_{mean}(E_b/N_0) = \sum_{k=0}^2 BER_k(E_b/N_0) \cdot P(D_{opt} = k) \quad (11)$$

The curve BER_{Dopt} of Figure 7 shows the BER of a system which synchronizes according to D_{opt} in Figure 6. This result can be reached by a system which synchronizes on each hop. In a second simulation we used the same radio channel for a system with a four times higher data rate ($T_b = 12.5 \mu s$). The results of the mean BER (BER_{mean}) according to (11) and the optimum BER (BER_{Dopt}) together with the previous results are depicted in Figure 8.

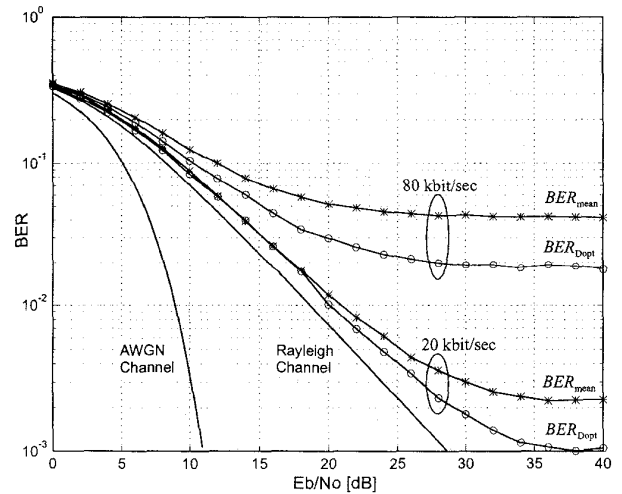


Figure 8: BER for different data rates

The results for the higher datarate (80 kbit/sec) are comparable to a 20 kbit transmission with a four times higher delay spread of the radio channel which also could be measured in this area (Figure 4) [Saf98].

CONCLUSION

We present a method to simulate the performance of a VHF-FH-radio in a multipath environment with a synthesized channel model taking into account the diffuse spatial distribution of partial waves. The simulation shows that the BER is strongly effected by the synchronization mechanism. For the given radio channel the irreducible error floor of a FH-system which randomly synchronizes at one frequency is two times higher compared with a system which synchronizes on each hop. For both systems, a four times higher datarate results in a twenty times higher BER.

ACKNOWLEDGMENT

The authors wish to thank Brigadier A. Knoll of the Austrian Ministry of Defense for his initiation and encouragement of this project that led to the presented paper.

REFERENCES

- [Bel63] P.A.Bello, „Characterisation of Randomly Time-Variant Linear Channels“, IEEE Trans. on Communication Syst., CS-11, pp. 360-393, 1963.
- [Ber97] G.Berger, H.Safer, Channel Sounder for the Tactical VHF-Range, IEEE Proceedings MILCOM, Monterey, pp. 1474-1478, November 2-5, 1997.
- [Ber98] G.Berger, H.Safer, F.Seifert, „Performance of VHF-FH-Radios with Different Bit-Synchronization Mechanisms in a Multipath Environment“, IEEE Proc. ISSSTA, 1998.
- [Bla95] J.J.Blanz, P.W.Baier, P.Jung, „A Flexibly Configurable Statistical Channel Model for Mobile Radio Syst. with Directional Diversity“, ITG-Fachb.135, VDE, pp. 93-100, 1995.
- [Bla96] J.J.Blanz, A.Klein, W.Mohr, „Measurement-based parameter adaption of wideband spatial mobile radio channel models“, IEEE Proc. ISSSTA, Mainz, pp. 91-97, 1996.
- [Jer92] M. C. Jeruchim, P. Balaban, K. S. Shanmugan, „Simulation of Communication Systems“, Plenum Press, 1992.
- [Saf98] H. Safer, G. Berger „Wideband Propagation Measurements of the VHF Mobile Radio Channel in different Areas of Austria“, IEEE Proceedings ISSSTA, Sun City, 1998.